Supporting Information

Reactions of Transition Metal Carbyne Cations with Ethylene in the Gas Phase

Xiao-Nan Wu*, Zizhuang Liu, Hechen Wu, Di Zhang, Wei Li, Zejian Huang, Guanjun Wang, Fuxing Xu, Chuan-fan Ding and Mingfei Zhou*

Department of Chemistry, Collaborative Innovation Center of Chemistry for Energy Materials, Shanghai Key Laboratory of Molecular Catalysis and Innovative Materials, Fudan University, Shanghai 200433, China. Email: wuxiaonan@fudan.edu.cn, mfzhou@fudan.edu.cn

Complete Ref. (27) Frisch, M. J.; Trucks, G. W.; Schlegel, H. B.; Scuseria, G. E.; Robb, M. A.; Cheeseman, J. R.; Scalmani, G.; V. Barone; Mennucci, B.; Petersson, G. A.; Nakatsuji, H.; Caricato, M.; Li, X.; Hratchian, H. P.; Izmaylov, A. F.; Bloino, J.; Zheng, G.; Sonnenberg, J. L.; Hada, M.; Ehara, M.; Toyota, K.; Fukuda, R.; Hasegawa, J.; Ishida, M.; Nakajima, T.; Honda, Y.; Kitao, O.; Nakai, H.; Vreven, T.; Montgomery Jr., J. A.; Peralta, J. E.; Ogliaro, F.; Bearpark, M.; Heyd, J. J.; Brothers, E.; Kudin, K. N.; Staroverov, V. N.; Kobayashi, R.; Normand, J.; Raghavachari, K.; Rendell, A.; Burant, J. C.; Iyengar, S. S.; Tomasi, J.; Cossi, M.; Rega, N.; Millam, J. M.; Klene, M.; Knox, J. E.; Cross, J. B.; Bakken, V.; Adamo, C.; Jaramillo, J.; Gomperts, R.; Stratmann, R. E.; Yazyev, O.; Austin, A. J.; Cammi, R.; Pomelli, C.; Ochterski, J. W.; Martin, R. L.; Morokuma, K.; Zakrzewski, V. G.; Voth, G. A.; Salvador, P.; Dannenberg, J. J.; Dapprich, S.; Daniels, A. D.; Farkas, Ö.; Foresman, J. B.; Ortiz, J. V.; Cioslowski, J.; Fox, D. J., Gaussian 09, Revision A.01, Gaussian, Inc., Wallingford CT, **2009**.

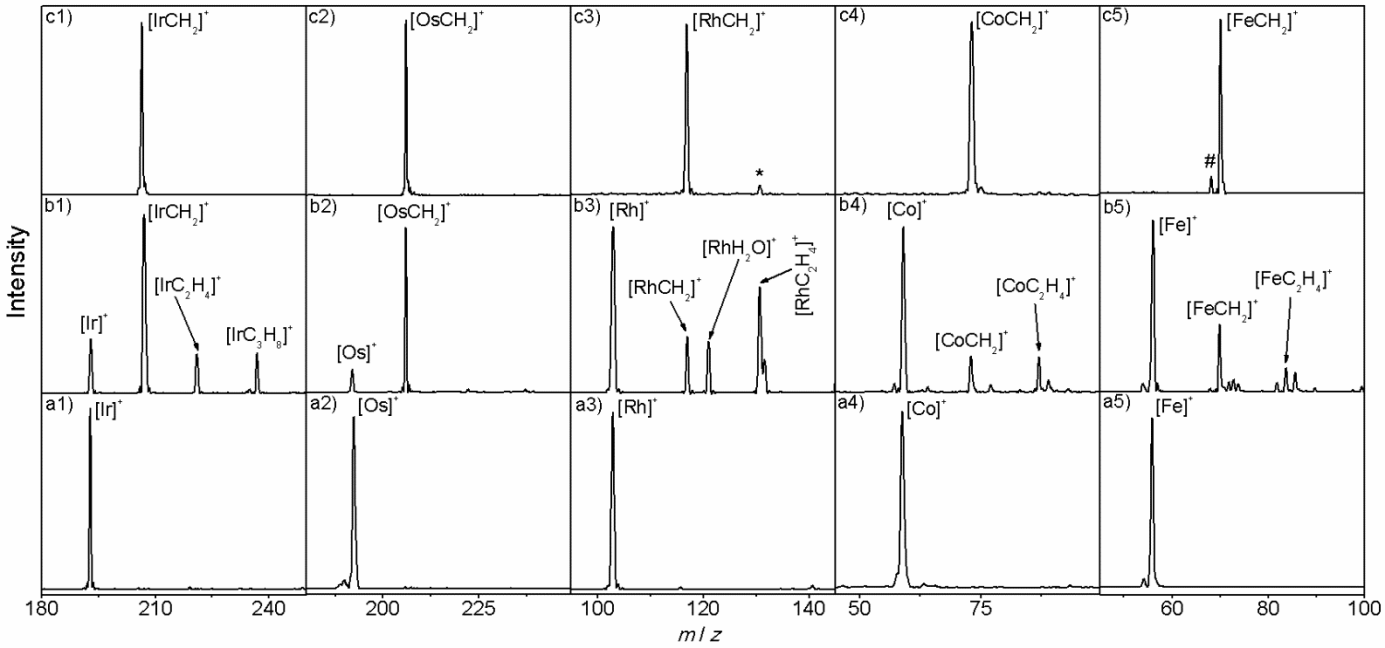

Figure S1. Mass spectra of mass-selected $[TM]^+$ (TM=Ir, Rh, Co, Os, Fe) (a1-a5). The bare metal ions react with CH_4 or C_2H_4O to form ions with mass spectra shown in b1 ($[Ir]^+$+CH_4), b2 ($[Rh]^+$+C_2H_4O), b3 ($[Co]^+$+C_2H_4O), b4 ($[Os]^+$+CH_4), and b5 ($[Fe]^+$+C_2H_4O). The $[TMCH_2]^+$ ions are mass-selected by the ion trap (shown in Figures c1-c5). The most abundance isotope is selected for $[Ir]^+$, $[Os]^+$, and $[Fe]^+$ ions (^{193}Ir, ^{192}Os, and ^{56}Fe).

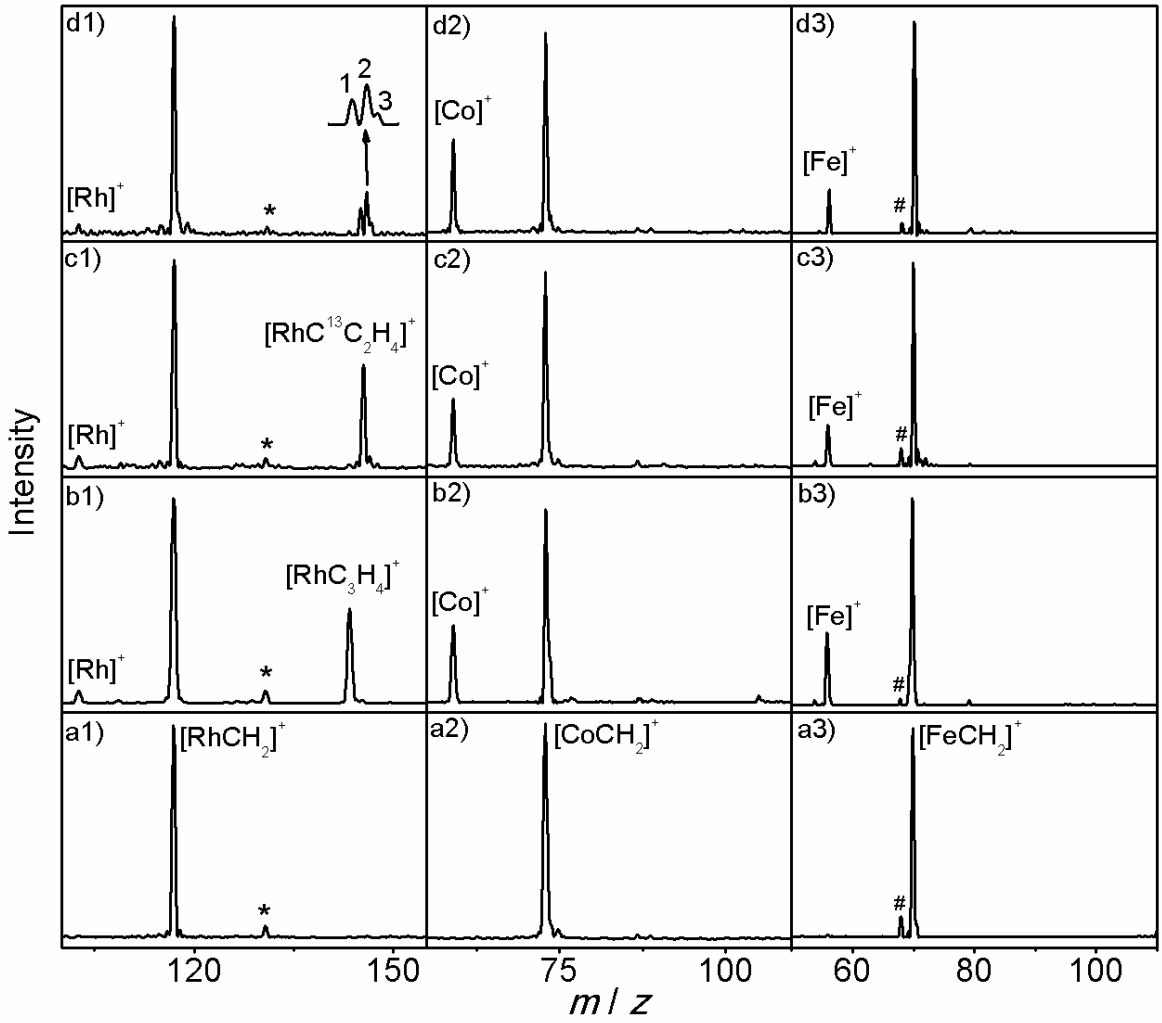

Figure S2. Mass spectra showing the reactions of $[TMCH_2]^+$ (TM = Rh, Co and Fe) with He (a1, a2 and a3), C_2H_4 (b1, b2 and b3), $^{13}C_2H_4$ (c1, c2 and c3), and C_2D_4 (d1, d2 and d3), respectively. **1**, **2** and **3** denote $[RhC_3H_2D_2]^+$, $[RhC_3HD_3]^+$ and $[RhC_3D_4]^+$ ions in Figure d1. The peaks marked with ∗ and # in Figures a1-d1 and a3-d3 are trace of $[RhC_2H_4]^+$ and $[^{54}FeCH_2]^+$.

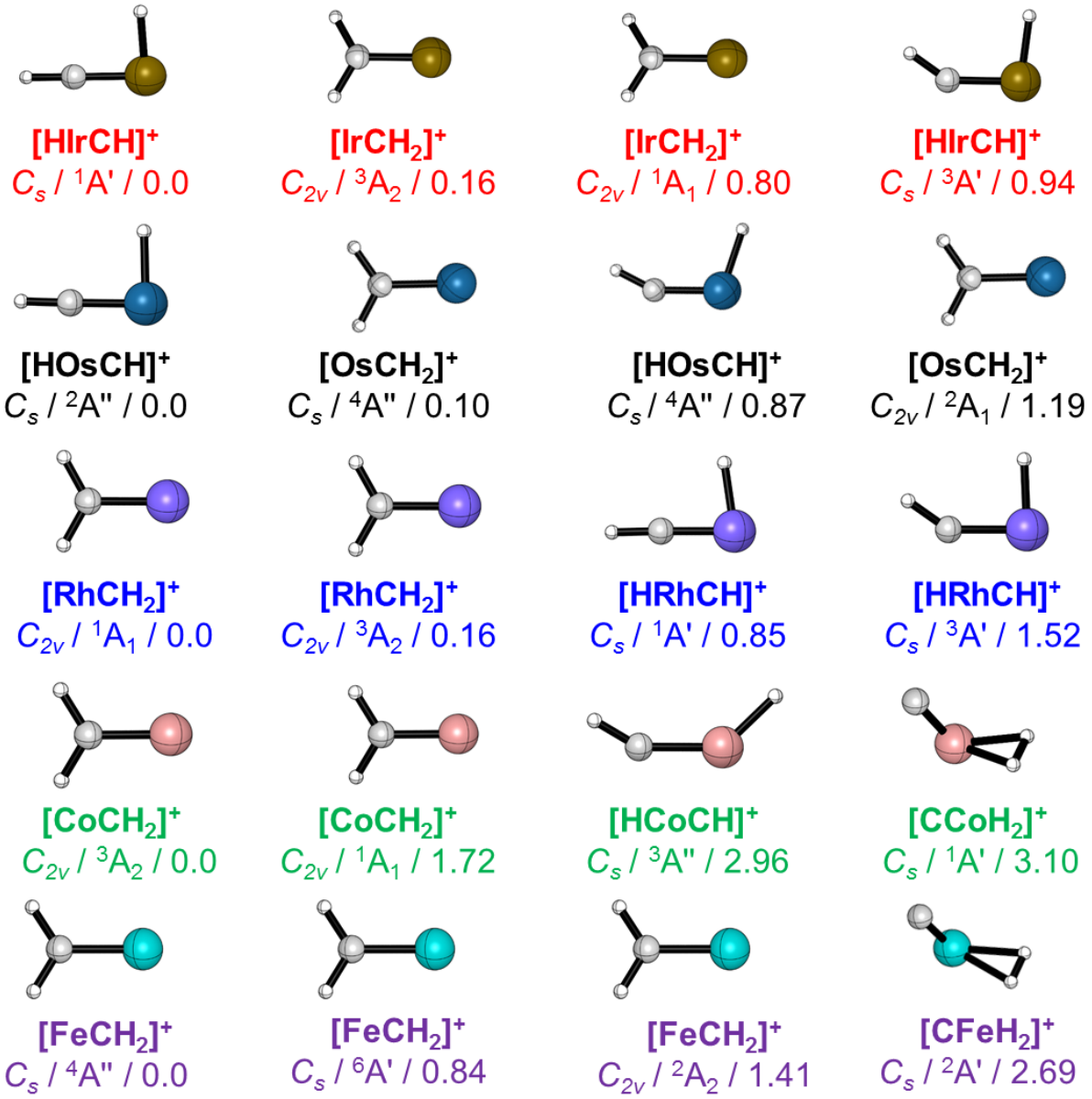

Figure S3: The predicted low-lying isomers of $[TMCH_2]^+$ (TM = Ir, Rh, Co, Os, and Fe). The relative energies are given in eV with respect to the most stable isomer.

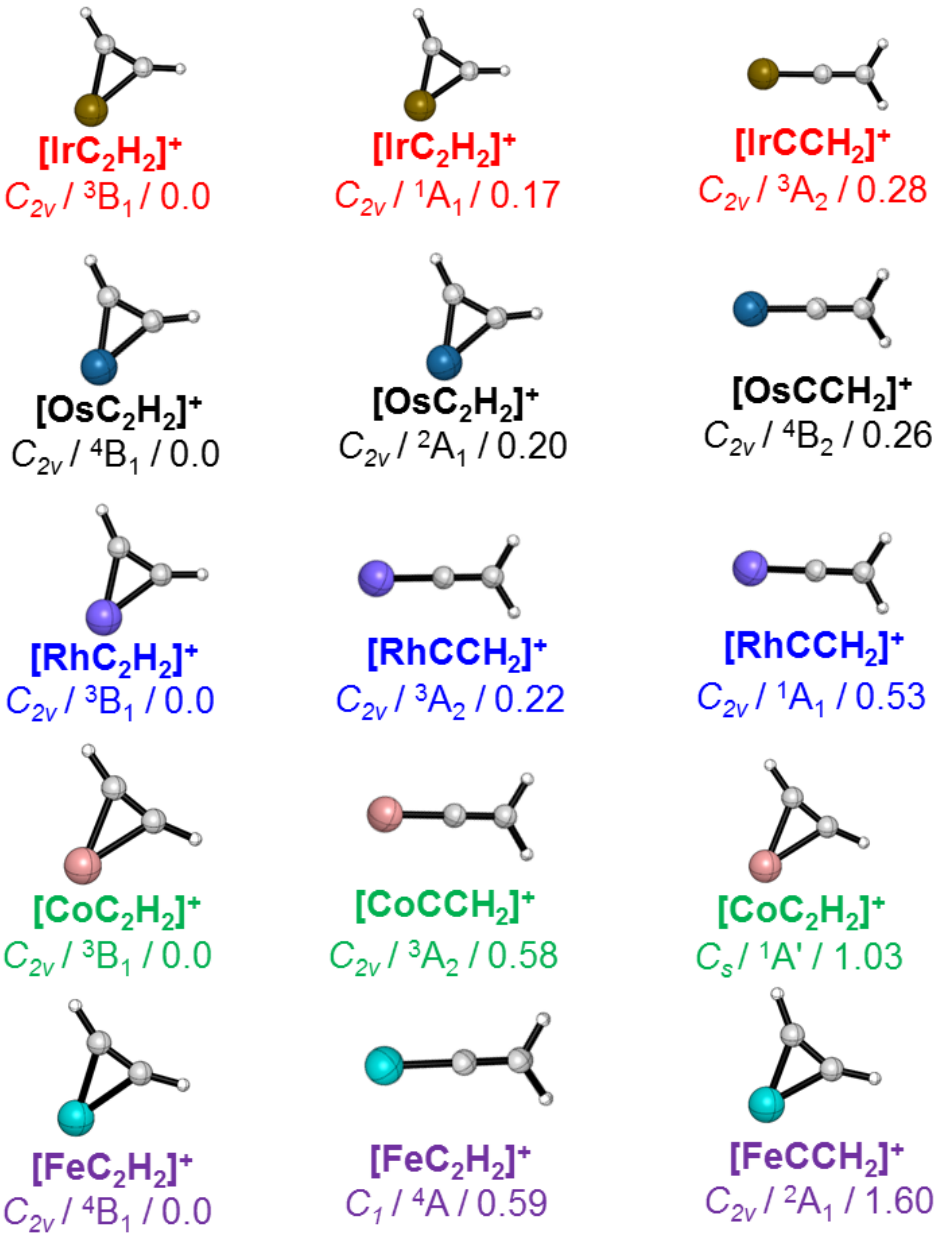

Figure S4: The predicted low-lying isomers of $[TMC_2H_2]^+$ (TM = Ir, Rh, Co, Os, and Fe). The relative energies are given in eV with respect to the most stable isomer.

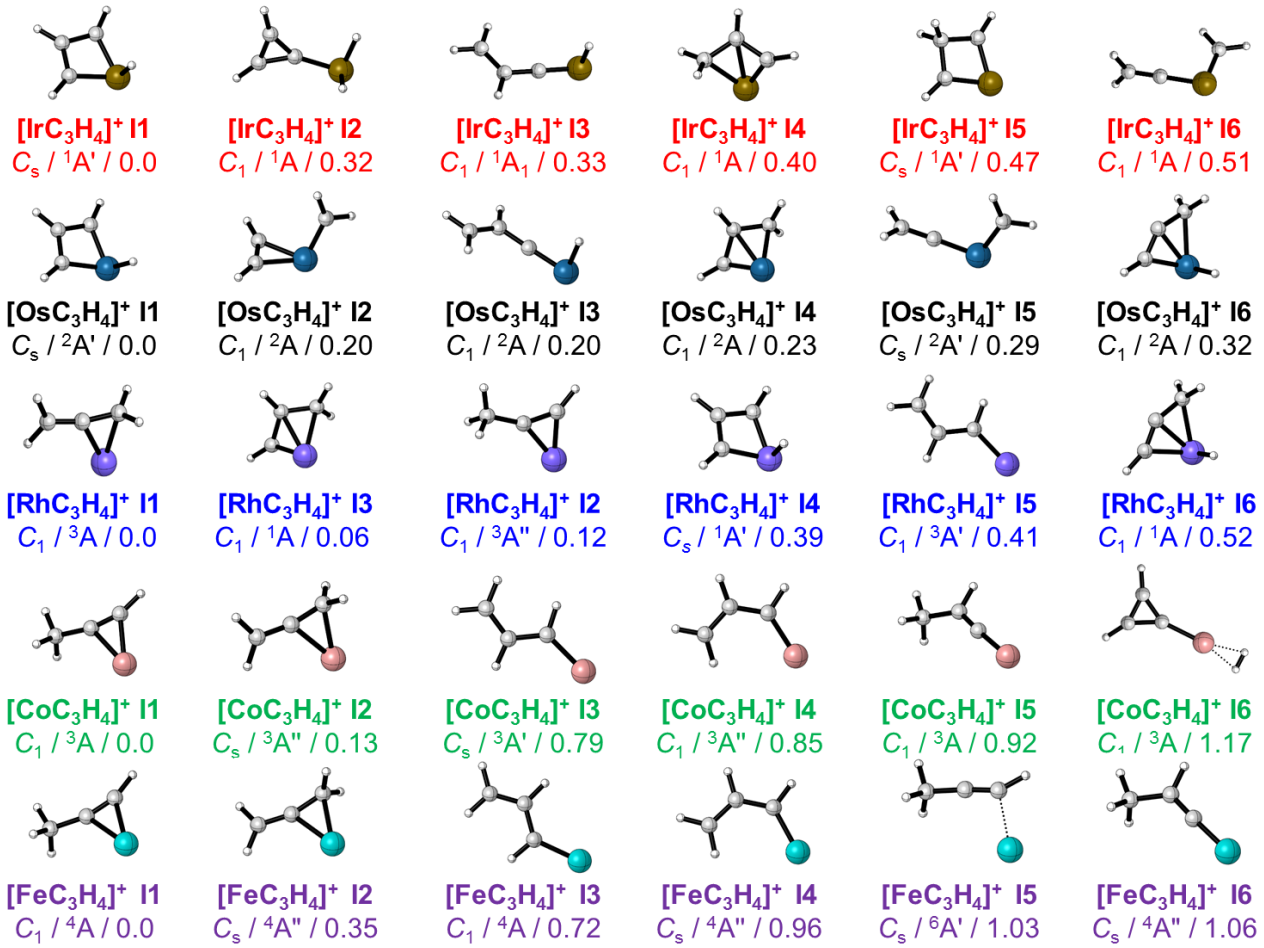

Figure S5: The predicted low-lying isomers of $[TMC_3H_4]^+$ (TM = Ir, Rh, Co, Os, and Fe). The relative energies are given in eV with respect to the most stable isomer.

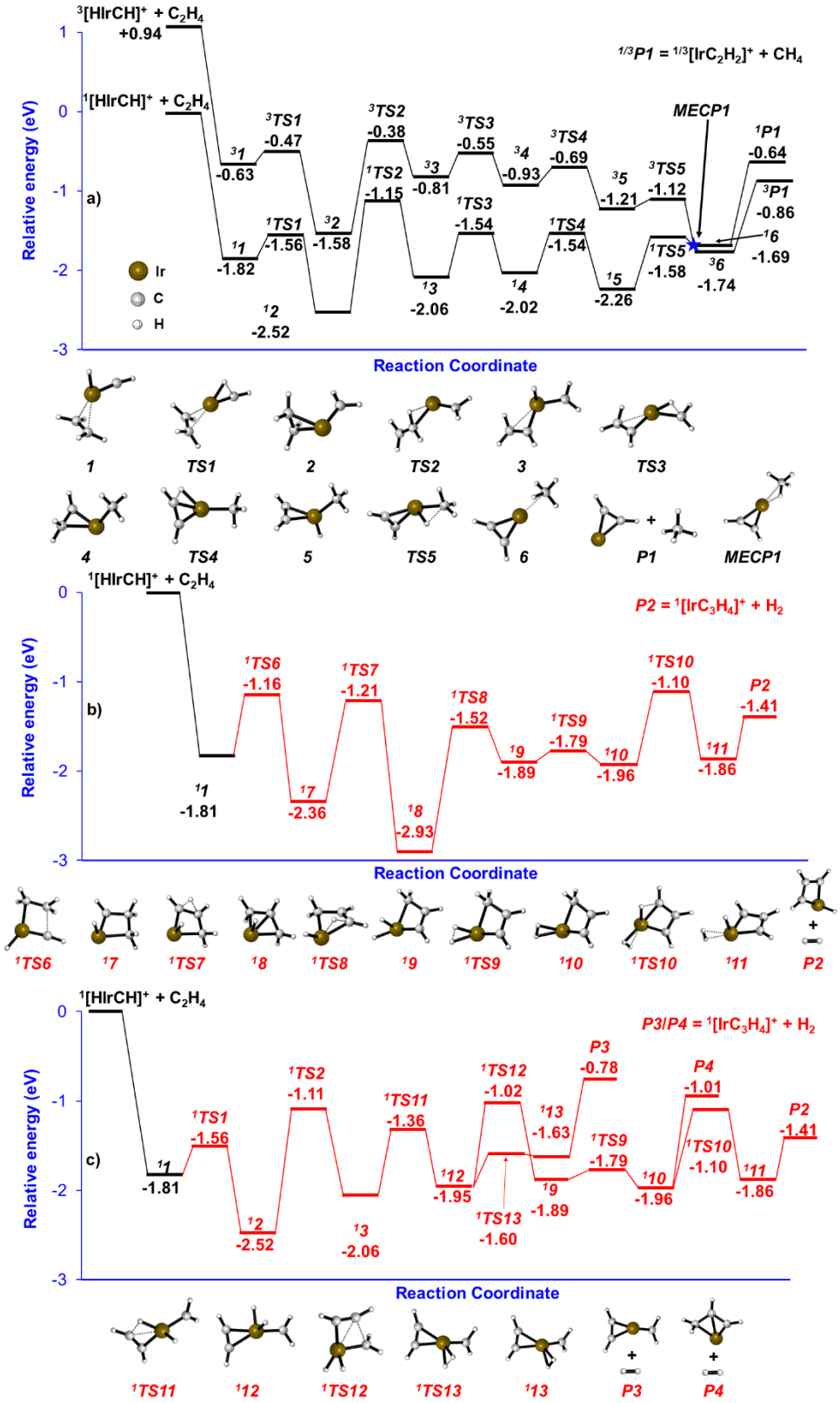

Figure S6. Potential energy profiles of the reaction of $[HIrCH]^+$ and C_2H_4. The energies are given in eV.

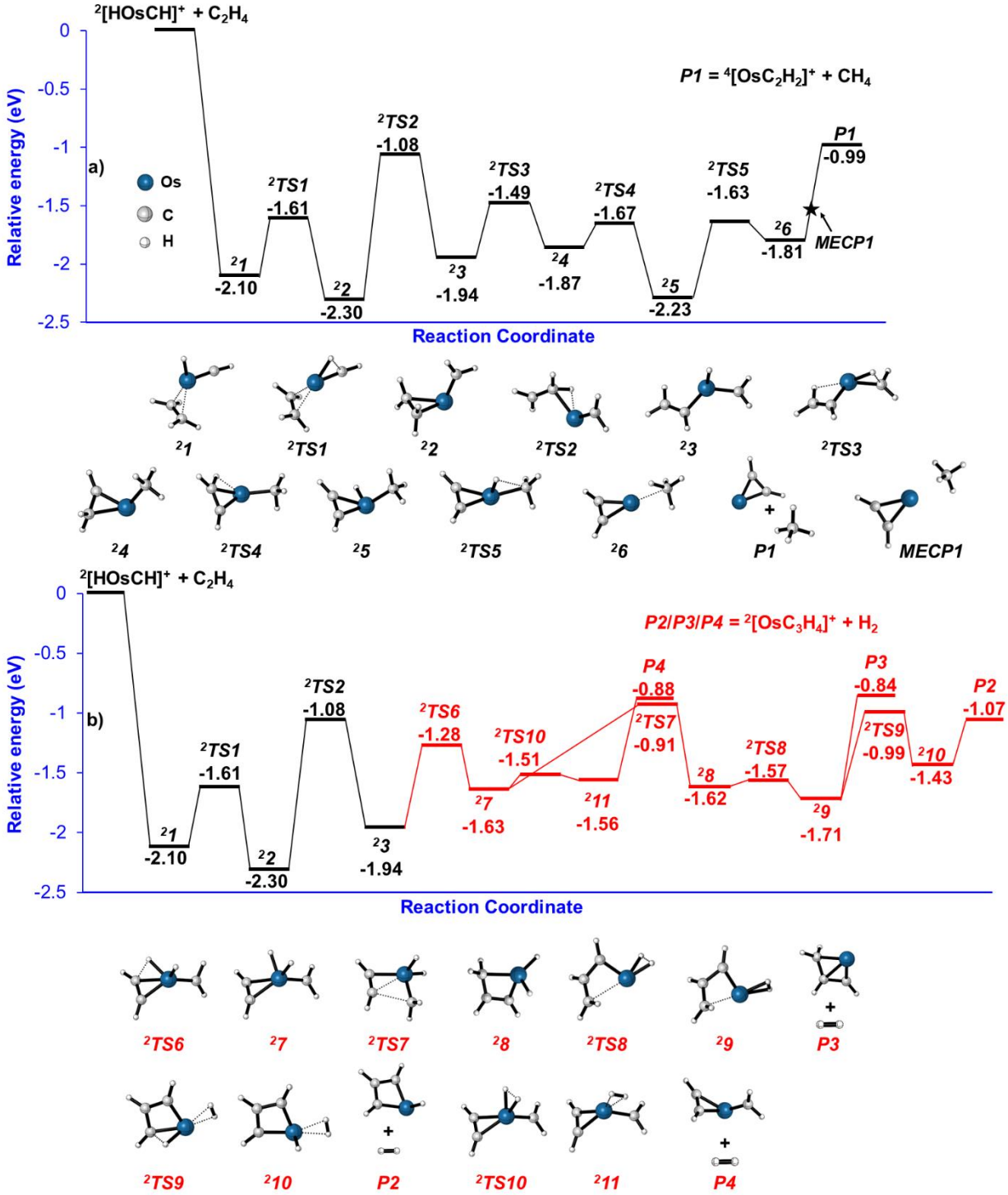

Figure S7. Potential energy profiles of the reaction of $[HOsCH]^+$ and C_2H_4. The energies are given in eV.

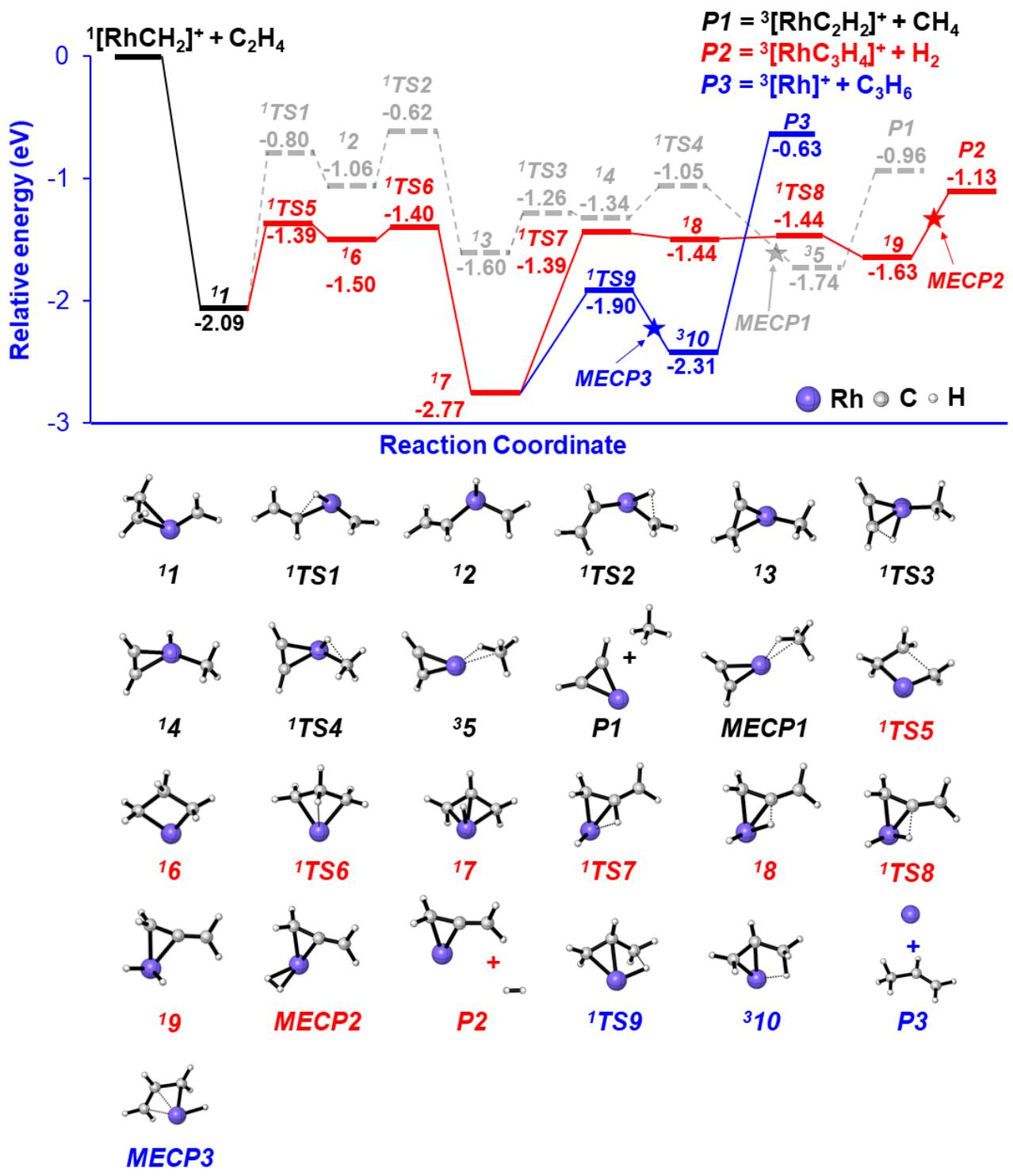

Figure S8. Potential energy profiles of the reaction of $[RhCH_2]^+$ and C_2H_4. The energies are given in eV.

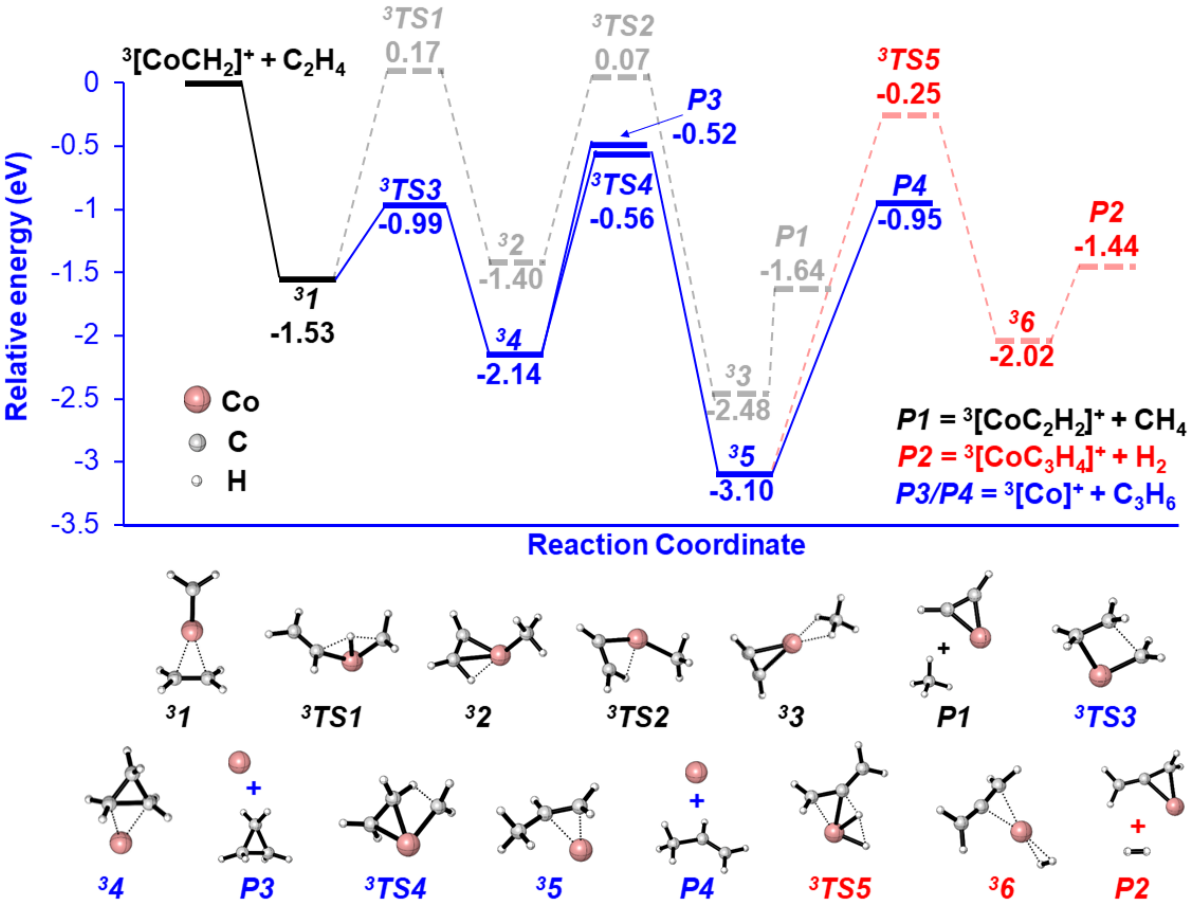

Figure S9. Potential energy profiles of the reaction of $[CoCH_2]^+$ and C_2H_4. The energies are given in eV.

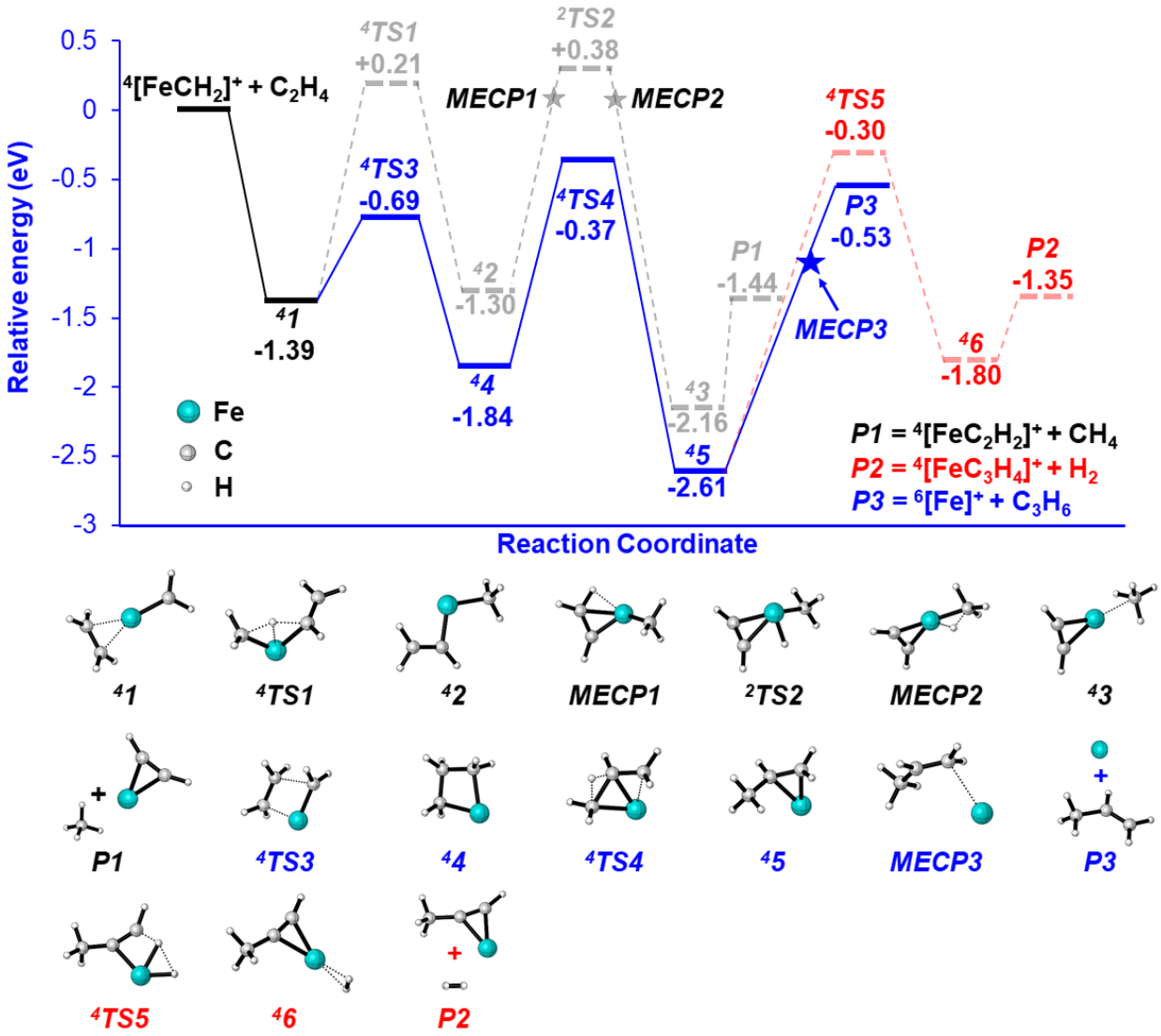

Figure S10. Potential energy profiles of the reaction of $[FeCH_2]^+$ and C_2H_4. The energies are given in eV.

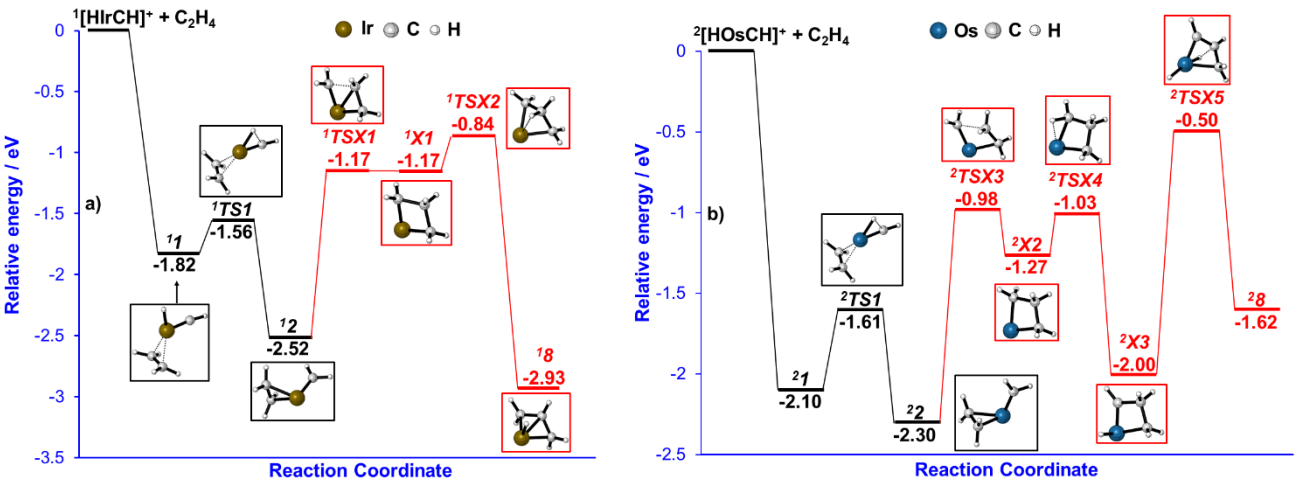

Figure S11. The reaction pathways from intermediates **2** to **8** for Ir (a) and Os (b).

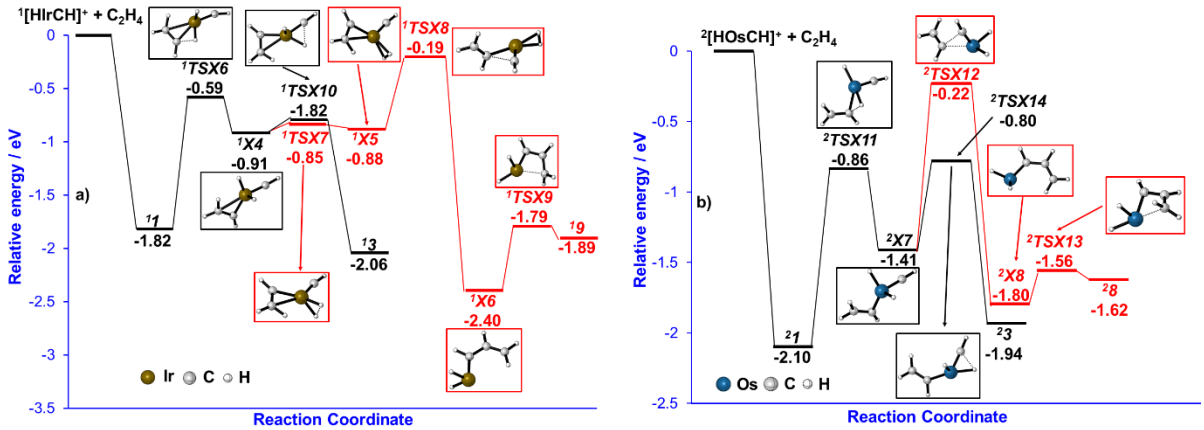

Figure S12. The reaction pathways for the direct dehydrogenation for Ir (a) and Os (b).

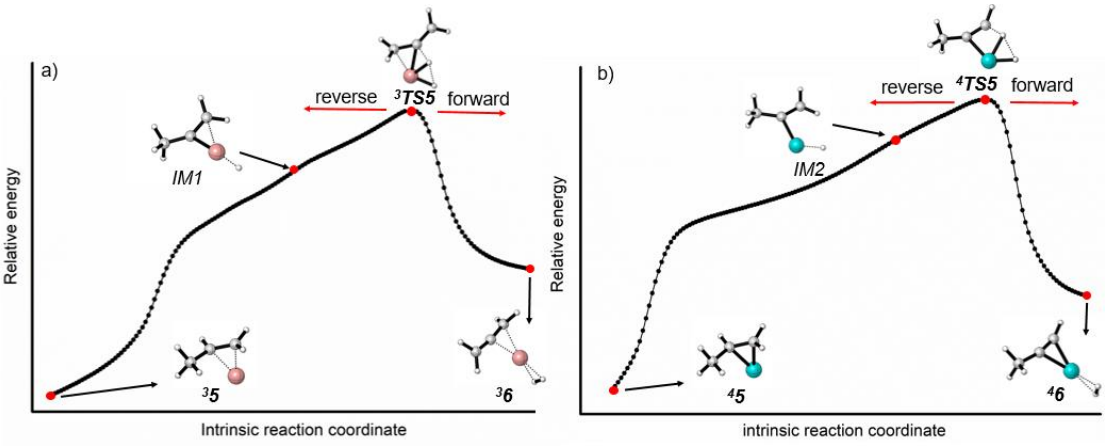

Figure S13. The IRC for the transition states ***³TS5*** in Figure S9 and ***⁴TS5*** in Figure S10.

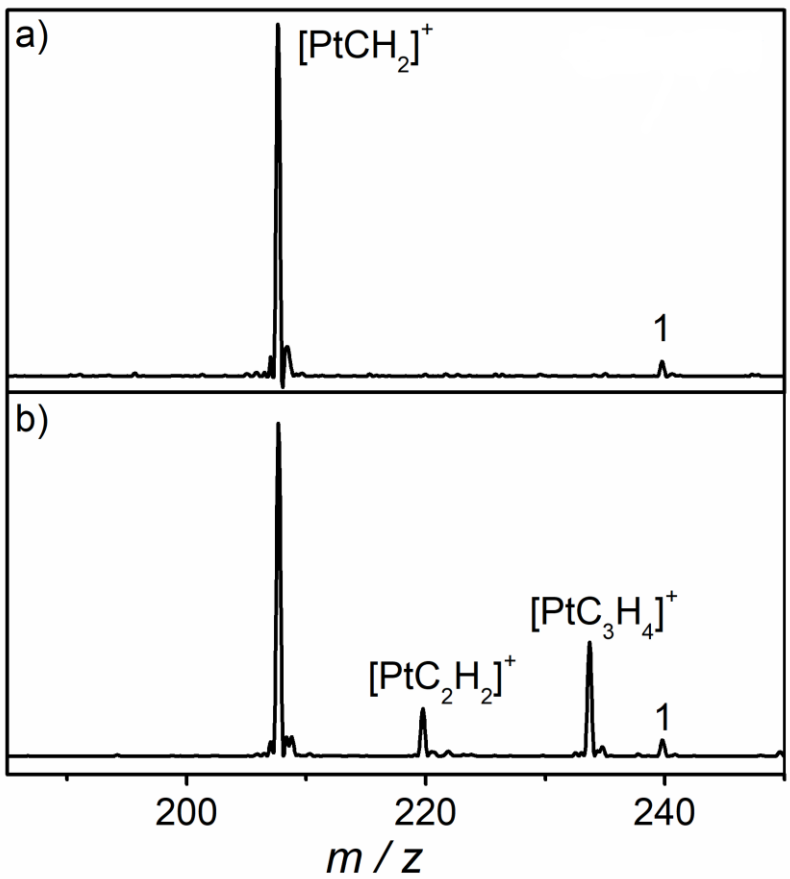

Figure S14. Mass spectra from the reactions of $[PtCH_2]^+$ with He (a) and C_2H_4 (b).